

Simulation of Upper Tropospheric CO₂ From Chemistry and Transport Models

Xun Jiang^{1*}, Qinbin Li¹, Mao-Chang Liang^{2,3}, Run-Lie Shia³, Moustafa T. Chahine¹,
Edward T. Olsen¹, Luke L. Chen¹, Jame Randerson⁴, and Yuk L. Yung³

¹ Science Division, Jet Propulsion Laboratory, California Institute of Technology, USA

² Research Center for Environmental Changes, Academia Sinica, Taipei, Taiwan.

³ Division of Geological and Planetary Sciences, California Institute of Technology, Pasadena, USA.

⁴ Department of Earth System Science, University of California, Irvine, USA.

* To whom all correspondence should be addressed. E-mail: xun@gps.caltech.edu

To be submitted to GBC, Jun 20, 2007

Abstract:

The Caltech/JPL two-dimensional (2-D), three-dimensional (3-D) GEOS-Chem, and 3-D MOZART-2 chemistry and transport models (CTMs), driven respectively by NCEP2, GEOS-4 and NCEP1 reanalysis data, have been used to simulate upper tropospheric CO₂ from 2000 to 2004. Model results of CO₂ mixing ratios agree well with aircraft observations at altitudes between 8 and 13 km [Matsueda *et al.*, 2002] in the tropics. The upper tropospheric CO₂ seasonal cycle phases are well captured by the CTMs. Model results have smaller seasonal cycle amplitudes in the southern hemisphere compared with those in the northern hemisphere, which are consistent with the aircraft data. Some discrepancies are evident between the model and aircraft data in the mid-latitudes, where models tend to underestimate the amplitude of CO₂ seasonal cycle. Comparison of the simulated vertical profiles of CO₂ between the different models reveals that the convection in the 3-D models is likely too weak in boreal winter and spring. Model sensitivity studies suggest that convection mass flux is crucial for the correct simulation of upper tropospheric CO₂. In addition, we found that the dominant inter-hemispheric change of CO₂ appears in the upper troposphere in the models. Thus the correct simulation of upper tropospheric CO₂ is essential for improving models that are used for deriving the surface sources and sinks from global measurements.

1. Introduction

[1] The increasing level of atmospheric CO₂ has significant influence on the global climate changes [Dickinson and Cicerone, 1986]. It is very difficult to disentangle the contributions from the different sources and sinks of atmospheric CO₂. Most inversions for the CO₂ sources and sinks are constrained by surface measurements [Fan *et al.*, 1998; Tans *et al.*, 1990; GLOBALVIEW-CO₂, 2002; Suntharalingam *et al.*, 2003; Gurney *et al.*, 2004]. For example, the global three-dimensional (3-D) inverse modeling analysis of surface flask and oceanic CO₂ measurements by Tans *et al.* [1990] implied a significant carbon sink in the northern hemisphere (NH) terrestrial biosphere. The inversion of carbon fluxes is very sensitive to CO₂ network configuration [Fan *et al.*, 1998; Suntharalingam *et al.*, 2002]. In addition, the inversion results are also very sensitive to the vertical transport in the tracer transport models [Law *et al.*, 1996; Fan *et al.*, 1998; Gurney *et al.*, 2004].

[2] Previous modeling studies [Randerson *et al.*, 1997; Kawa *et al.*, 2004] mainly focused on simulating the seasonal cycle and trend of surface CO₂. The upper tropospheric CO₂ concentrations, from *in situ* aircraft measurements, usually differ by ~5 ppmv relative to the surface concentrations [Anderson *et al.*, 1996; Nakazawa *et al.*, 1997]. Matsueda *et al.* [2002] has been measuring CO₂ mixing ratios biweekly since April 1993 aboard commercial airlines at 8-13 km altitudes over the western Pacific from Australia to Japan. This data set offers a unique opportunity to test the ability of chemistry and transport models (CTMs) in simulating the upper tropospheric CO₂. The retrievals of CO₂ mixing ratios from the Atmospheric Infrared Sounder (AIRS), with a high precision of ~1-2 ppmv [Chahine *et al.*, 2005], provide a spaceborne global perspective on the upper tropospheric CO₂. The retrievals can be used for constraining the vertical transport in CTMs [Chahine *et al.*, 2007].

[3] Using a two-dimensional (2-D) CTM, Shia *et al.* [2006] successfully simulated the seasonal cycle and trend of CO₂ in the upper troposphere. In this study, we will investigate instead how well global 3-D CTMs are able to simulate the seasonal cycle and

trend of upper tropospheric CO₂. Surface emissions and vertical transport in CTMs are both very crucial for the correct simulation of CO₂. We will use two different boundary conditions to investigate the contribution of boundary conditions to the upper tropospheric CO₂. One is a boundary condition where the CO₂ surface mixing ratios are constructed with measurements from the Climate Monitoring and Diagnostics Laboratory (CMDL) surface network. The other is with prescribed known CO₂ sources and sinks. To investigate the influence of vertical transport, we will compare results from GEOS-Chem and MOZART-2 with four different vertical transport schemes.

2. Models and Data

[4] The Caltech/JPL 2-D CTM [*Shia et al.*, 2006], 3-D GEOS-Chem [*Suntharalingam et al.*, 2003], and 3-D MOZART-2 [*Horowitz et al.*, 2003] are used to simulate CO₂. The 2-D CTM has 18 latitude boxes, equally spaced from pole to pole. It has 40 vertical layers, equally spaced in log (p) from the surface to the upper boundary at 0.01 hPa. Transport in the model is by the stream function and the horizontal and vertical diffusivities taken from *Jiang et al.* [2004]. The stream function is derived from the National Center for Climate Prediction (NCEP) Reanalysis 2 data [*Jiang et al.*, 2004]. For altitudes above 40 km where no NCEP data are available, we adopt the climatologically averaged circulation derived by *Fleming et al.* [2002]. There is a gradual merging of the two data sets between 30 and 40 km. An important feature of the 2-D CTM is its ability to reproduce the age of air in the stratosphere [*Morgan et al.*, 2004].

[5] GEOS-Chem (v7.3.3) is driven by the Goddard Earth Observing System (GEOS-4) assimilated meteorological data from the NASA Global Modeling Assimilation Office (GMAO). For the computational consideration, we regridded the GEOS-4 data into 2° (latitude) × 2.5° (longitude) in horizontal and 30 levels in vertical. It extends from the surface to about 0.01 hPa (~70 km). Advection is computed every 15 minutes with a flux-form semi-Lagrangian method [*Lin and Rood*, 1996]. Moist convection is computed using the GEOS convective, entrainment, and detrainment mass fluxes described by *Allen et al.* [1996a, 1996b]. The physics in the GEOS-4 analysis system are adopted from the

National Center for Atmospheric Research (NCAR) Community Climate Model, Version 3 (CCM3) and Whole Atmosphere Community Climate Model (WACCM) with important modifications to make it suitable for data assimilation [Bloom *et al.*, 2005]. The deep convection scheme is based on Zhang and McFarlane [1995]. The shallow convection treatment follows Hack [1994]. The planetary boundary layer turbulence parameterization is from Holtslag and Boville [1993]. To investigate the influence of different vertical mixings on the upper tropospheric CO₂, we also force the GEOS-Chem model with the GEOS-3 reanalysis data, which employs the Relaxed Arakawa Schubert convection parameterization [Moorthi and Suarez, 1992].

[6] MOZART-2 is driven by the meteorological inputs every 6 hours from the NCEP Reanalysis 1 [Kalnay *et al.*, 1996]. Advection is computed every 20 minutes with a flux-form semi-Lagrangian method [Lin and Rood, 1996]. The horizontal resolution is 2.8° (latitude) × 2.8° (longitude) with 28 vertical levels extending up to approximately 40 km altitude [Horowitz *et al.*, 2003]. MOZART-2 is built on the framework of the Model of Atmospheric Transport and Chemistry (MATCH). MATCH includes representations of advection, convective transport, boundary layer mixing, and wet and dry deposition. Penetrative convection in the NCEP Reanalysis 1 is described by Pan and Wu [1994], which is based on Arakawa and Schubert [1974] as simplified by Grell [1993] with a saturated downdraft. Shallow convection from NCEP Reanalysis 1 is determined by Tiedtke [1983]. We also forced MOZART-2 with meteorological data from the middle atmosphere version of NCAR Community Climate Model (MACCM3), which has the same convective scheme as the GEOS-4 Reanalysis. We found the CO₂ results from MOZART-2 forced by MACCM3 meteorological fields are very close to that from GEOS-Chem driven by GEOS-4 data, so we defer the detailed discussion to a separate study.

[7] The CMDL CO₂ mixing ratio data [Tans *et al.* 1998; GLOBALVIEW-CO₂, 2002] are used in this study as the lower boundary condition for the Caltech/JPL CTM, GEOS-Chem, and MOZART-2. For convenience, we refer this hereforth as the CMDL boundary condition. We assume that all atmospheric CO₂ originates from the surface layer is

practically chemically inert in the atmosphere considering its long lifetime. With the CMDL boundary condition, discrepancy between model results and observations would help diagnose potential issues with model transport. However, we noticed that the CMDL surface stations are sparse in the southern hemisphere (SH), and that the CMDL boundary condition is also biased toward oceanic sites. In a separate simulation using GEOS-Chem, we use prescribed CO₂ sources and sinks as the boundary condition, as described in *Suntharalingam et al.* [2003]. The exchange of CO₂ between the terrestrial biosphere and atmosphere is based on the net primary productivity from *Randerson et al.* [1997]. Air-to-sea exchange of CO₂ is from *Takahashi et al.* [1997]. Estimates of fossil fuel emissions are from *Andres et al.* [1996]. Monthly mean biomass burning emissions of CO₂ are derived based on *Duncan et al.* [2003]. Discrepancies between the GEOS-Chem CO₂ simulations (driven by the same GEOS-4 reanalysis data) with the abovementioned two boundary conditions would help identify potential issues with the surface sources and/or sinks.

[8] Table 1 summarizes the different model experiments as discussed in Section 3. Model results will be compared with aircraft measurements from *Matsueda et al.* [2002] and CMDL [*GLOBALVIEW-CO₂*, 2002].

3. Results

[9] Figures 1 and 2 compare the aircraft observations of CO₂ averaged between 8 and 13 km (red dots) [*Matsueda et al.*, 2002] and model results averaged at the same altitude range for 2000-2004. The panels are for 35°S to 35°N latitudes in 10° steps. The amplitudes of the seasonal cycle of CO₂ are smaller in the SH than those in the NH, for there is less contribution from the seasonal cycle in the vegetation photosynthesis. The green line shows results from a GEOS-Chem simulation driven by GEOS-4 data using the CMDL boundary condition (Experiment A in Table 1), which agrees well with the aircraft data. The orange line is GEOS-Chem CO₂ (driven by GEOS-4 data) with prescribed sources and sinks (Experiment B). Results from these two simulations are generally consistent. Because the transport is the same in both experiments, difference in

the results may reflect deficiencies in the prescribed sources/sinks in Experiment B. In general, CO₂ concentrations from Experiment B are larger than those from Experiment A in the NH from July to October, especially at 35°N. This implies a possible missing terrestrial sink in the NH in Experiment B. The GEOS-Chem CO₂ forced by the GEOS-3 meteorological fields and the CMDL boundary condition (pink line; Experiment C) and CO₂ from MOZART-2 (blue line) both agrees very well with the aircraft data. Experiment C includes only results for 2000-2002, as GEOS-3 data are available for only up to 2002.

[10] The agreement between the 3-D model results (solid lines) and aircraft data is fairly good, except at the NH mid-latitudes, where the 3-D models underestimate the amplitude of the seasonal cycle of CO₂ as seen in the aircraft data. Similar results are found by comparing the model results to the CMDL aircraft CO₂ data at Carr (40.9°N, 104.8°W) and Poker Flat (65.07°N, 147.29°W) as shown in the Figs. A1-A2 of the auxiliary material. In fact, the models all tend to underestimate the seasonal cycles of CO₂ in the middle to high latitudes.

[11] To investigate this problem, we plotted the vertical profiles of CO₂ simulated by each model at 5°N (upper panel) and 35°N (lower panel) of 2003 in Figure 3. In the tropics (5°N) the 3-D model results closely follow that from the 2-D model. As alluded to in Section 2, the 2-D model has been “tuned” to reproduce the distribution of tracers [see, *e.g.*, Appendix A of *Morgan et al.*, 2004]. In the northern mid-latitudes (35°N), all 3D models seem to underestimate the upper tropospheric CO₂ in January and April of 2003.

[12] To quantitatively compare the trend and seasonal cycle of CO₂ between the aircraft data and model results, a multiple regression method is applied to CO₂. We decompose CO₂ concentrations by the empirical model consisting of the first, second, and third Legendre functions and the harmonic functions of seasonal cycle and semi-annual cycles [*Prinn et al.*, 2000]:

$$X(t) = a + bNP_1(t/N - 1) + 1/3cN^2P_2(t/N - 1) + 1/5dN^3P_3(t/N - 1) + e \cos(2\pi t) + f \sin(2\pi t) + g \cos(4\pi t) + h \sin(4\pi t) \quad (1)$$

where t is from 0 to the $2N$ year (whole time period); P_1 , P_2 , and P_3 are the first, second, and third Legendre functions. The coefficients a , b , and c are the mean value, the trend, the acceleration in the trend, and the coefficient for P_3 , respectively. We add the third Legendre function to better fit the data sets. e and f are the amplitudes of the annual cycle. g and h are the amplitudes of the semi-annual cycle.

[13] Raw CO₂ data from the aircraft measurements and model experiments at 35°N are shown as red dots and solid lines respectively in Figure 4. Dashed lines are the sum of all terms in the right hand side of Eq. (1), which fit well with the raw aircraft data and model results. We then detrended the data by subtracting the sum of the first three Legendre functions. The results are very close to remove a third order polynomials. The detrended aircraft data in the four years are shown as red dots in Figs. 5 and 6. Diamond and error bar are the mean and standard deviation of the detrended aircraft data for each month. Black dotted line is the sum of the annual and semi-annual cycles terms in Eq. (1), which follows well the monthly mean aircraft data (Diamonds). For comparison, we also detrended the model results using the same method. Then we composited the detrended model CO₂ from all four years. Results are shown as solid lines in Figs. 5 and 6. The phase of CO₂ seasonal cycle is well captured by the different model simulations. The seasonal cycle amplitude is larger in the NH than that in the SH, which is captured by all models. Most 3-D models underestimate the seasonal cycle amplitude in the NH.

[14] Linear trend (b) and seasonal cycle amplitude ($\sqrt{e^2 + f^2}$) for CO₂ are listed in Table 2. Most models seem to capture the CO₂ trend correctly in the NH. In the SH, the agreement is not as good and most probably due to the poor representation of the SH dynamics in GCMs [Kalnay *et al.*, 1996]. The trend of CO₂ is smaller in MOZART-2 than those from GEOS-Chem and the 2D CTM, which may be due to the different trends in the different transport fields. With more observations available in the future, the CO₂ trend can be defined more accurately. The latitudinal distribution of CO₂ seasonal cycle amplitude is shown in Fig. 7. Because of the short simulation time period in Experiment C, we do not include it in Fig. 7. All 3-D models underestimate the amplitude of CO₂

seasonal cycle in the NH mid-latitudes. The seasonal cycle amplitude of upper tropospheric CO₂ in the 2-D CTM is larger than those from the 3-D models. The amplitude of CO₂ seasonal cycle is larger in MOZART-2 than those in GEOS-Chem. The GEOS-Chem simulation forced by the CMDL boundary condition (Experiment A) has a larger CO₂ seasonal cycle than the GEOS-Chem simulation forced by surface sources and sinks (Experiment B), which indicates a possible missing terrestrial sink in the NH. GEOS-Chem CO₂ (Experiments A and B) overestimate the seasonal cycle amplitude in the SH, which may be due to the biases in the SH transport in GEOS-4.

[15] To further explore the role of different parameters for simulating CO₂ correctly in the upper troposphere, sensitivity studies have been conducted using the GEOS-Chem model driven by GEOS-4 reanalysis data and the CMDL boundary condition. We first perturbed the turbulent mixing in the planetary boundary layer by 50% (Experiment F). The resulting differences between the perturbed run (Experiment F) and control run (Experiment A) are shown in Fig. 8a. The CO₂ concentrations differ by less than ~0.04 ppmv at altitudes below 3.5 km, a rather small effect. We also perturbed separately the convective updraft mass flux by 20% (Experiment G). The resulting differences between the perturbed run (Experiment G) and control run (Experiment A) are shown in Fig. 8b. The largest increase of ~0.65 ppmv in CO₂ is found at 6 km, which is very significant for simulating the upper tropospheric CO₂.

[16] Accurate simulation of CO₂ concentrations in the upper troposphere is also imperative for deducing the interhemispheric transport of CO₂. It is generally accepted that the NH is a net CO₂ source and the SH (the oceans) is a net CO₂ sink [IPCC, 2001]. However, it is not clear at what altitude most of the transport of CO₂ from the NH to the SH takes place. Figure 9 shows the altitude dependence of the zonal averaged, annual mean CO₂ mixing ratios from GEOS-Chem (Experiment A) and the Caltech 2-D CTM (Experiment D) for 2003. There is clearly a net NH to SH transport, and a large component of this transport occurs in the upper troposphere, which is consistent with previous studies by other tracers [Prather *et al.*, 1987; Prinn *et al.*, 1992]. Therefore, correctly modeling upper tropospheric CO₂ takes on added significance. Consider a flux

inversion in which CO₂ in the NH was not efficiently transported to the upper troposphere, resulting in less transport to the SH and a lower calculated southern ocean sink. This would create artificially high CO₂ in the NH, demanding a large land sink to reconcile the model predictions with the observations.

4. Conclusions

[17] 2-D and 3-D chemistry and transport models, driven by different transport schemes, have been used to simulate the upper tropospheric CO₂ from 2000 to 2004. We also apply different boundary conditions to force the 3-D CTMs. We found that the influence of the boundary layer on the upper tropospheric CO₂ is less important compared with different transport schemes. Model CO₂ agree generally well with the aircraft data from 35°S to 35°N. The trends of CO₂ are simulated correctly by most of the models. The phases of CO₂ seasonal cycles are also captured well by models. Similar to those in the aircraft data, model CO₂ have a smaller seasonal cycle amplitudes in the SH compared with those in the NH. However, 3-D CTMs appear to underestimate the seasonal cycle amplitude of upper tropospheric CO₂ in the NH mid-latitudes. Sensitivity studies reveal that the convective mass fluxes are very crucial for simulating the upper tropospheric CO₂. In both 2D CTM and 3D GEOS-chem models there is a net CO₂ transport from NH to SH, occurring mainly in the upper troposphere. This suggests that the accurate simulation of upper tropospheric CO₂ is very important for deducing the correct inter-hemispheric flux of CO₂. In addition to the aircraft data, global AIRS CO₂ data will become available in the near future [Chahine *et al.*, 2007]; global total column CO₂ data will be available in two years [Crisp *et al.*, 2004]. These data can be used to constrain the vertical and horizontal transport in the CTMs, resulting in more realistic models. This will give us greater confidence in deducing sources and sinks of CO₂ using a combination of global CO₂ data and inverse modeling [Miller *et al.*, 2007].

Acknowledgement: This work is performed at JPL under contract with NASA, and is supported by project 01STHR/04.2.03.3. Our special thanks to Bob Yantosca at Harvard University for the help on the GEOS-Chem model and to Peter Hess, Larry Horowitz, and Jean-Francois Lamar on the MOZART-2 model. R. L. Shia and Y. L. Yung are supported by NSF grant ATM-9903790. M.C. Liang also would like to acknowledge the support from an NSC grant 95-2111-M-001-009 to the Academia Sinica.

References:

- Allen, D. J., R. B. Rood, A. M. Thompson, and R. D. Hidson (1996a), Three-dimensional ^{222}Rn calculations using assimilated data and a convective mixing algorithm, *J. Geophys. Res.*, *101*, 6871-6881.
- Allen, D. J., *et al.* (1996b), Transport induced interannual variability of carbon monoxide using a chemistry and transport model, *J. Geophys. Res.*, *101*, 28655-28670.
- Anderson, B. E. *et al.* (1996), Airborne observations of spatial and temporal variability of tropospheric carbon dioxide, *J. Geophys. Res.*, *101*(D1), 1985-1997.
- Andres, R. J., G. Marland, I. Fung, and E. Matthews (1996), Distribution of carbon dioxide emissions from fossil fuel consumption and cement manufacture, 1950-1990, *Global Biogeochem. Cycles*, *10*, 419-429.
- Arakawa, A., and W. H. Shubert (1974), Interaction of a cumulus ensemble with the large-scale environment, Part I, *J. Atmos., Sci.*, *31*, 674-704.
- Bloom, S., *et al.* (2005), The Goddard Earth Observation System Data Assimilation System, GEOS DAS Version 4.0.3: Documentation and Validation, NASA TM-2005-104606, 26, 166pp.
- Chahine, M., *et al.*, (2005), On the determination of atmospheric minor gases by the method of vanishing partial derivatives with application to CO_2 , *Geophys. Res. Lett.*, *32*(22), L22803.
- Chahine, M., *et al.*, (2007), Space observations of mid-tropospheric CO_2 and correlation with ground sources, manuscript in preparation.
- Crisp, D., *et al.*, (2004), The orbiting carbon observatory (OCO) mission, *Advances in Space Research*, *34*, 700-709.
- Dickinson, R. E., and R. J. Cicerone (1986), Future global warming from atmospheric trace gases, *Nature*, *319*(6049), 109-115.
- Duncan, B. N., *et al.* (2003), Interannual and seasonal variability of biomass burning emissions constrained by satellite observations, *J. Geophys. Res.*, *108*, doi:10.1029/2002JD002378.
- Fan, S., *et al.* (1998), A large terrestrial carbon sink in North America implied by atmospheric and oceanic CO_2 data and models, *Science*, *282*, 442-446.
- Fleming, E. L., *et al.* (2002), Two-dimensional model simulations of the QBO in ozone and tracers in the tropical stratosphere, *J. Geophys. Res.*, *107*, doi:10.1029/2001JD001146.
- GLOBALVIEW- CO_2 (2002), *Cooperative Atmospheric Data Integration Project: Carbon Dioxide* [CD-ROM], Clim. Monit. and Diagnostics Lab., NOAA, Boulder, Colo. (<http://www.cmdl.noaa.gov/ccgg/globalview/co2/index.html>)
- Grell, G. A. (1993), Prognostic evaluation of assumptions used by cumulus parameterizations, *Mon. Wea. Rev.*, *121*, 764-787.
- Gurney, K. R. *et al.* (2004), Transcom 3 inversion intercomparison: Model mean results for the estimation of seasonal carbon sources and sinks, *Global Biogeochem. Cycles*, *18*(1), GB1010.
- Kalnay, E., *et al.* (1996), The NCEP/NCAR 40-year reanalysis project, *Bull. Am. Meteorol. Soc.*, *77*, 437-471.

- Kawa, S. R., *et al.* (2004), Global CO₂ transport simulations using meteorological data from the NASA data assimilation system, *J. Geophys. Res.*, *109*, doi:10.1029/2004JD004554.
- Hack, J. J. (1994), Parameterization of moist convection in the NCAR community climate model (CCM2), *J. Geophys. Res.*, *99*, 5551-5568.
- Holtslag, A., and B. Boville (1993), Local versus nonlocal boundary-layer diffusion in a global climate model, *J. Clim.*, *6*, 1825-1842.
- Horowitz, L. W., *et al.* (2003), A global simulation of tropospheric ozone and related tracers: description and evaluation of MOZART, version 2, *J. Geophys. Res.*, *108*, doi:10.1029/2002JD002853.
- IPCC (2001), *IPCC Third Assessment Report (TAR): Climate Change 2001*, Intergovernmental Panel on Climate Change.
- Jiang, X. C. D. Camp, R. Shia, D. Noone, C. Walker, and Y. L. Yung (2004), Quasi-biennial oscillation and quasi-biennial oscillation-annual beat in the tropical total column ozone: A two-dimensional model simulation, *J. Geophys. Res.*, *109*, Art. No. JD004377.
- Law, R., *et al.* (1996), Variations in modeled atmospheric transport of carbon dioxide and the consequences for CO₂ inversions, *Global Biogeochem. Cycles*, *10*, 783-796.
- Lin, S. J., and R. B. Rood (1996), Multidimensional flux form semi-Lagrangian transport schemes, *Mon. Weather Rev.*, *124*, 2046-2070.
- Matsueda, H., H. Y. Inoue, and M. Ishii (2002), Aircraft observation of carbon dioxide at 8-13 km altitude over the western Pacific from 1993 to 1999, *Tellus*, *54B*(1), 1-21. The data are available at <http://gaw.kishou.go.jp/wdcgg.html>
- Miller, C. E., *et al.* (2007), Precision requirements for space-based Xco₂ data, *J. Geophys. Res.*, *112*, doi:10.1029/2006JD007659.
- Moorthi, S., and M. J. Suarez (1992), Relaxed Arakawa-Schubert – A parameterization of moist convection for general circulation models, *Mon. Wea. Rev.*, *120*(6), 978-1002.
- Morgan, C. G., *et al.* (2004), Isotopic fractionation of nitrous oxide in the stratosphere: Comparison between model and observations, *J. Geophys. Res.*, *109*, D04305.
- Nakazawa, T., *et al.* (1997), Aircraft measurements of the concentrations of CO₂, CH₄, N₂O, and CO and the carbon and oxygen isotopic ratios of CO₂ in the troposphere over Russia, *J. Geophys. Res.*, *102*, 3843-3859.
- Pan, H. L., and W. S. Wu (1994), Implementing a mass flux convection parameterization package for the NMC medium-range forecast model, *NMC office note*, No. 409, 40pp.
- Prather, M., *et al.* (1987), Chemistry of the global troposphere: Fluorocarbons as tracers of air motion, *J. Geophys. Res.*, *92*, 6579-6613.
- Prinn, R. G., *et al.* (1992), Global average concentration and trend for hydroxyl radicals deduced from ALE/GAGE trichloroethane (methylchloroform) data for 1978-1990, *J. Geophys. Res.*, *97*, 2445-2461.
- Prinn, R. G., *et al.* (2000), A history of chemically and radiatively important gases in air deduced from ALE/GAGE/AGAGE, *J. Geophys. Res.*, *105*, 17751-17792.
- Randerson, J. T., *et al.* (1997), The contribution of terrestrial sources and sinks to trends in the seasonal cycle of atmospheric carbon dioxide, *Global Biogeochem. Cycles*, *11*, 535-560.

- Shia, R., M. Liang, C. E. Miller, and Y. L. Yung (2006), CO₂ in the upper troposphere: influence of stratosphere-troposphere exchange, *Geophys. Res. Lett.*, *33*, doi:10.1029/2006GL026141.
- Suntharalingam, P., *et al.* (2003), Estimating the distribution of terrestrial CO₂ sources and sinks from atmospheric measurements: sensitivity to configuration of the observation network, *J. Geophys. Res.*, *108*, doi:10.1029/2002JD002207.
- Takahashi, T., *et al.* (1997), Global air-sea flux of CO₂: An estimate based on measurements of sea-air pCO₂ difference, *Proc. Natl. Acad. Sci. U. S. A.*, *94*, 8929.
- Tans, P. P., I. Y. Fung, and T. Takahashi (1990), Observational constraints on the global atmospheric CO₂ budget, *Science*, *247* (4949): 1431-1438.
- Tans, P.P., *et al.* (Eds.) (1998), Carbon Cycle, in *Climate Monitoring and Diagnostics Laboratory No. 24 Summary Report 1996-1997*, edited by D.J. Hoffmann *et al.*, chap. 2, pp. 30-51, NOAA Environ. Res. Lab., Boulder Colo. (Data available from <http://www.cmdl.noaa.gov/>)
- Tiedtke, M. (1983), The sensitivity of the time-mean large-scale flow to cumulus convection in the ECMWF model, *ECMWF workshop on convection in large-scale models*, Reading, England, pp. 297-316.
- Zhang, G. J., and N. A. McFarlane (1995), Sensitivity of climate simulations to the parameterization of cumulus convection in the Canadian climate centre general circulation model, *Atmos. Ocean*, *33*, 407-446.

Figure Captions:

Figure 1: Aircraft observations between 8 km and 13 km (red dots) [Matsueda *et al.*, 2002] and modeled CO₂ mixing ratios averaged at the same layer from 2000 to 2004. The panels are for 35°S, 25°S, 15°S, and 5°S, respectively. The CO₂ mixing ratios from the GEOS-Chem model (Experiments A, B, and C) are shown by the green, orange, and pink lines, respectively. The CO₂ mixing ratios from the Caltech-JPL 2-D model (Experiment D) are shown by purple lines. The CO₂ mixing ratios from MOZART-2 (Experiment E) are shown by the blue lines.

Figure 2: Aircraft observations between 8 km and 13 km (red dots) [Matsueda *et al.*, 2002] and modeled CO₂ mixing ratios averaged at the same layer from 2000 to 2004. The panels are for 5°N, 15°N, 25°N, and 35°N, respectively.

Figure 3: Vertical profiles of CO₂ in January, April, July, and October 2003. Colors are the same as in Figure 1. Upper panel: Latitude = 5°N. Lower panel: Latitude = 35°N.

Figure 4: CO₂ from aircraft and models at 35°N. Red dots are aircraft observations. Solid lines are model results. Colors are the same as in Figure 1. Dashed lines are the fit to the CO₂ (see text).

Figure 5: CO₂ seasonal cycles from detrended aircraft (Red dots) and detrended model results at 25°S, 15°S, and 5°S. Trends are determined by the sum of the first three legendre polynomials. Diamond and the error bar are the mean and standard deviation of the detrended aircraft data within each month.

Figure 6: CO₂ seasonal cycles from detrended aircraft (Red dots) and detrended model results at 5°N, 15°N, 25°N, and 35°N. Trends are determined by the sum of the first three legendre polynomials. Diamond and error bar are the mean and standard deviation of the detrended aircraft data within each month.

Figure 7: Latitudinal distribution of CO₂ seasonal cycle amplitude.

Figure 8: (a) CO₂ difference between the enhanced turbulence mixing in the planetary boundary layer simulation and control experiment. (b) CO₂ difference between the enhanced convective updraft mass flux simulation and control experiment.

Figure 9: (a) Longitudinally averaged CO₂ from 3D GEOS-Chem (Experiment A) for 2003. (b) CO₂ from 2D CTM (Experiment D) for 2003.

Table 1: Description of Model Experiments.

	Model	Transport	Boundary Condition	Model Change
Experiment A	3-D GEOS-Chem	GEOS-4	CMDL	
Experiment B	3-D GEOS-Chem	GEOS-4	CO ₂ sources and sinks	
Experiment C	3-D GEOS-Chem	GEOS-3	CMDL	
Experiment D	2-D Caltech/JPL CTM	NCEP2 and UKMO	CMDL	
Experiment E	3-D MOZART2	NCEP1	CMDL	
Experiment F	3-D GEOS-Chem	GEOS-4	CMDL	Increase turbulence mixing in the PBL by 50%
Experiment G	3-D GEOS-Chem	GEOS-4	CMDL	Increase the convective updraft mass flux by 20%

Table 2: Trend and Seasonal Cycle Amplitude of CO₂ From Matsueda Aircraft data and Model Simulations.

	Trend (ppmv/yr)							
	35°S	25°S	15°S	5°S	5°N	15°N	25°N	35°N
Aircraft		2.14±0.05	2.14±0.03	1.97±0.03	1.96±0.03	1.99±0.03	2.01±0.06	1.99±0.1
Experiment A	1.99±0.03	2.06±0.03	2.06±0.03	2.07±0.03	2.03±0.03	2.02±0.03	2.0±0.03	1.99±0.03
Experiment B	1.89±0.04	1.90±0.04	1.94±0.04	1.91±0.04	1.99±0.04	2.0±0.03	1.95±0.03	1.95±0.03
Experiment C	1.78±0.05	1.82±0.05	1.88±0.06	1.89±0.06	1.54±0.08	1.53±0.06	1.57±0.04	1.68±0.03
Experiment D	1.97±0.02	1.99±0.03	2.0±0.03	2.02±0.03	2.0±0.03	2.03±0.03	2.05±0.03	2.08±0.03
Experiment E	1.78±0.02	1.8±0.02	1.82±0.02	1.84±0.02	1.82±0.02	1.81±0.02	1.80±0.02	1.81±0.02
	Seasonal Cycle Amplitude (ppmv)							
Aircraft		0.38±0.14	0.38±0.08	0.90±0.08	1.61±0.08	2.05±0.09	2.47±0.17	2.48±0.3
Experiment A	0.28±0.06	0.95±0.08	1.03±0.1	0.74±0.08	1.21±0.07	1.64±0.06	1.61±0.06	1.51±0.07
Experiment B	0.57±0.08	0.7±0.09	0.74±0.1	0.57±0.1	1.17±0.07	1.5±0.07	1.3±0.06	1.32±0.07
Experiment C	0.1±0.08	0.64±0.07	0.83±0.1	0.52±0.1	1.24±0.11	1.98±0.09	2.06±0.06	1.87±0.05
Experiment D	0.21±0.05	0.49±0.07	0.66±0.08	1.06±0.07	1.44±0.07	1.94±0.07	2.33±0.07	2.36±0.08
Experiment E	0.28±0.05	0.58±0.05	0.64±0.06	0.77±0.06	1.30±0.05	1.88±0.06	1.90±0.07	1.88±0.06

Figure 2:

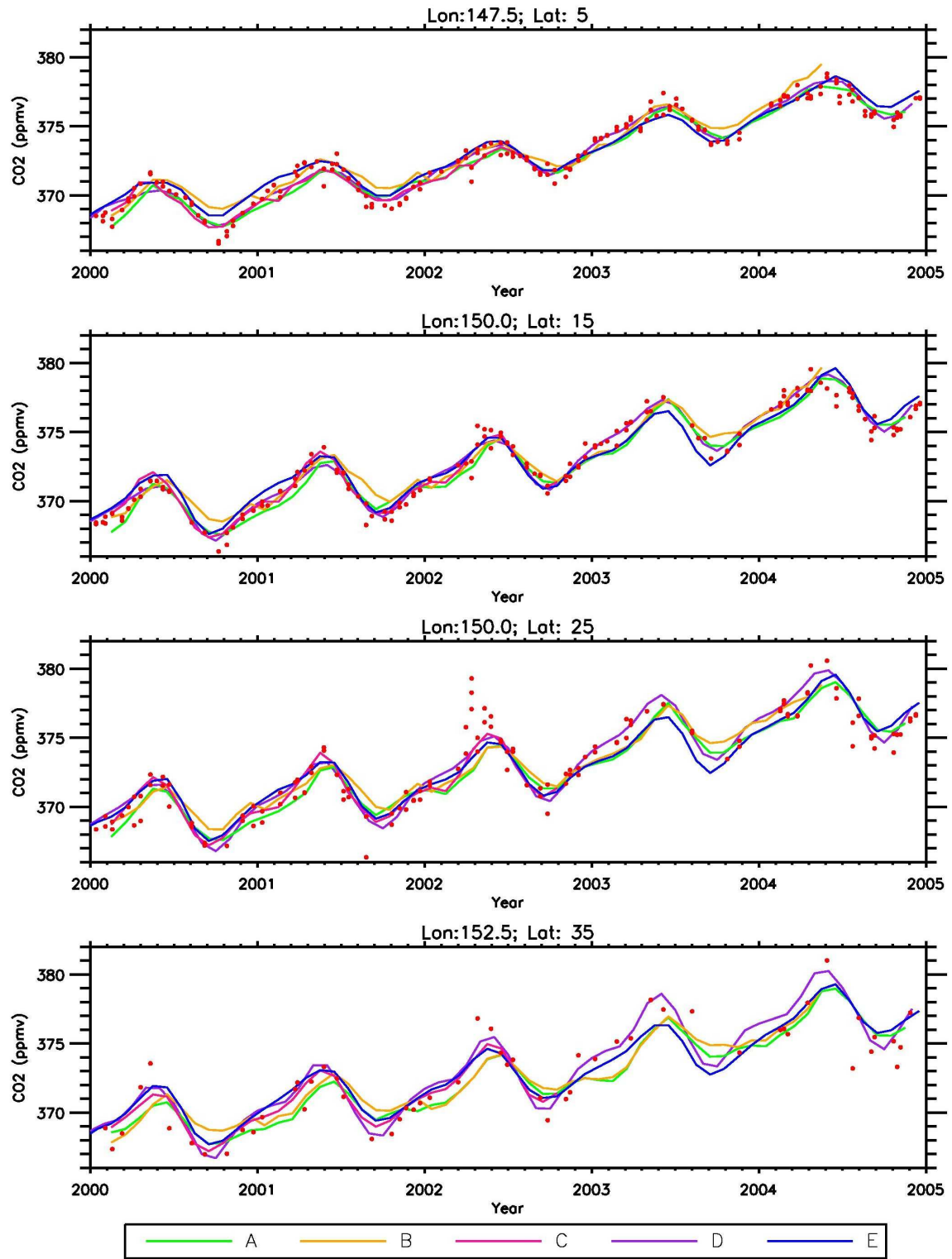


Figure 3:

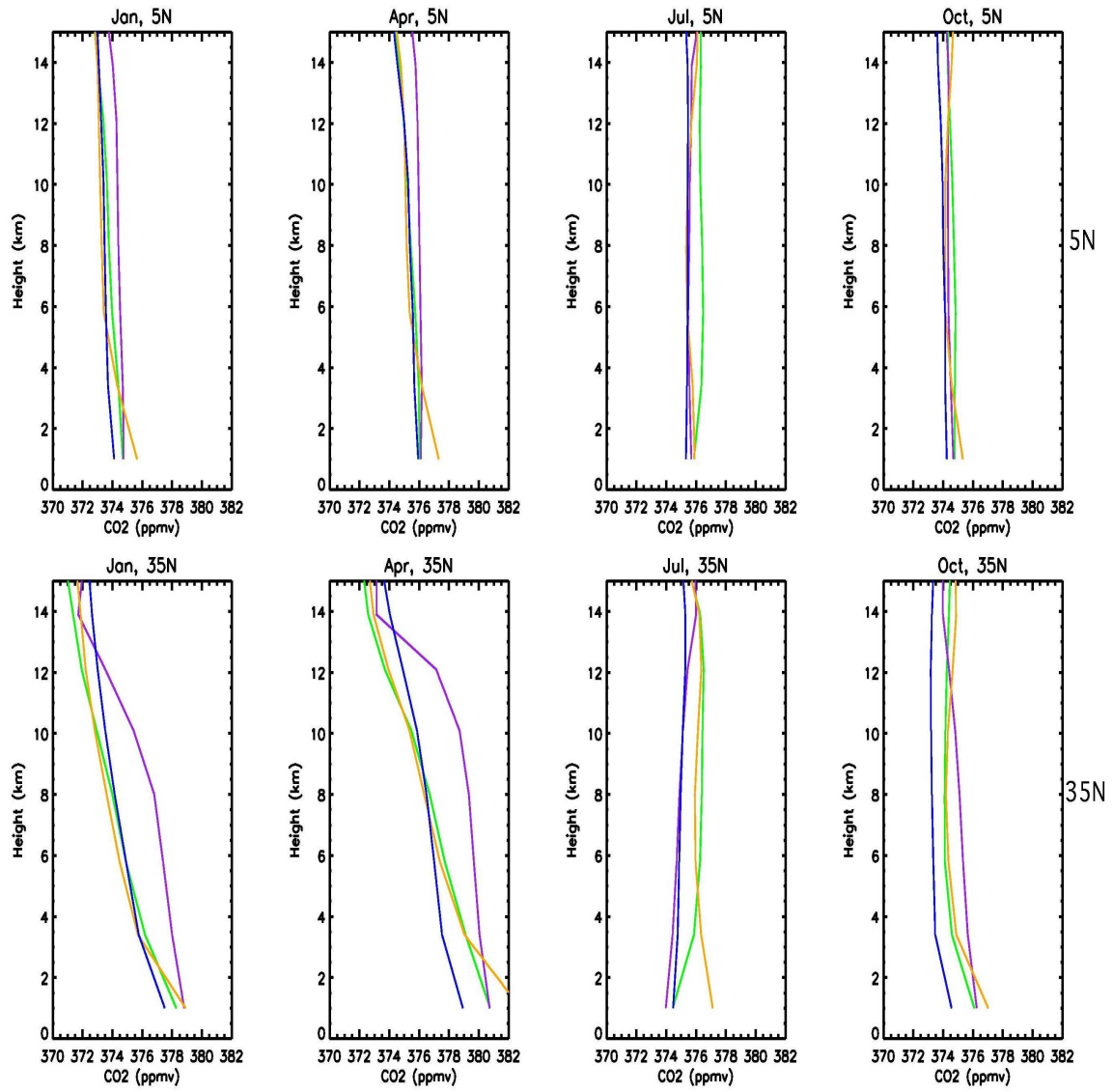


Figure 4:

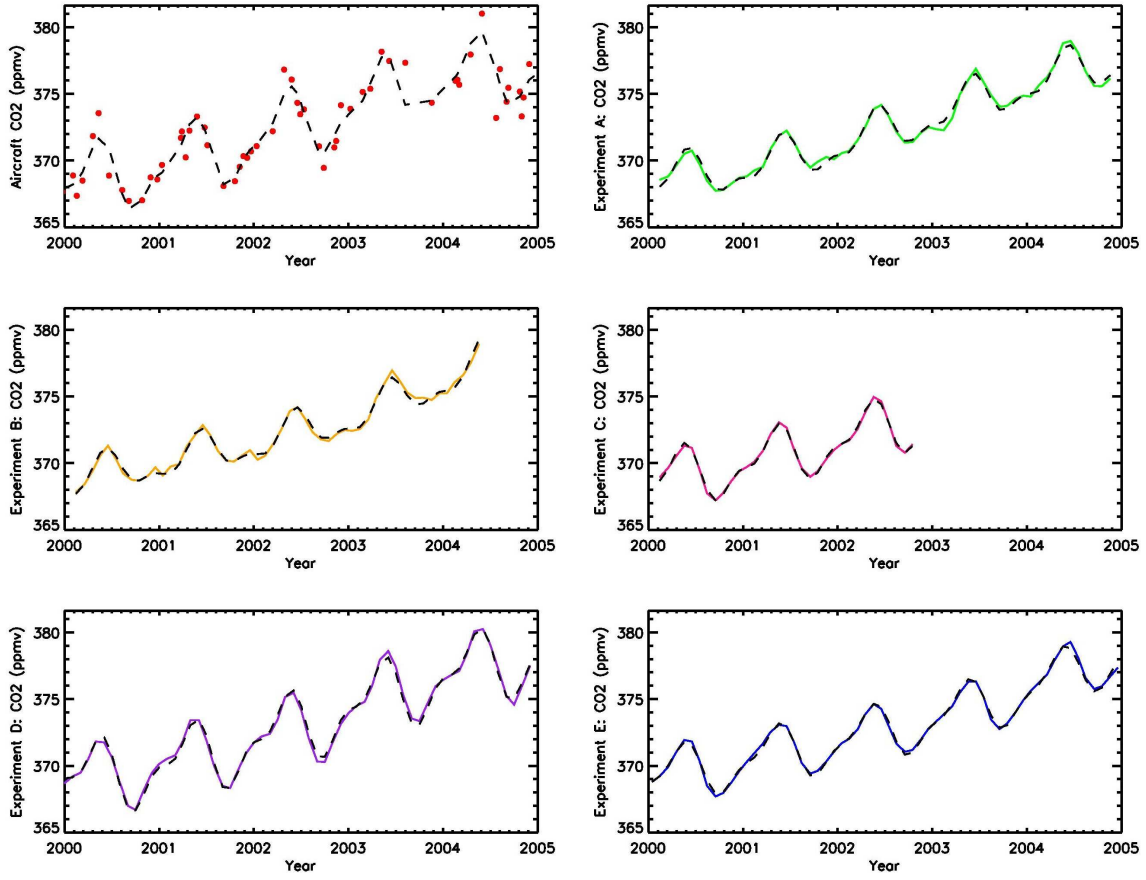


Figure 5:

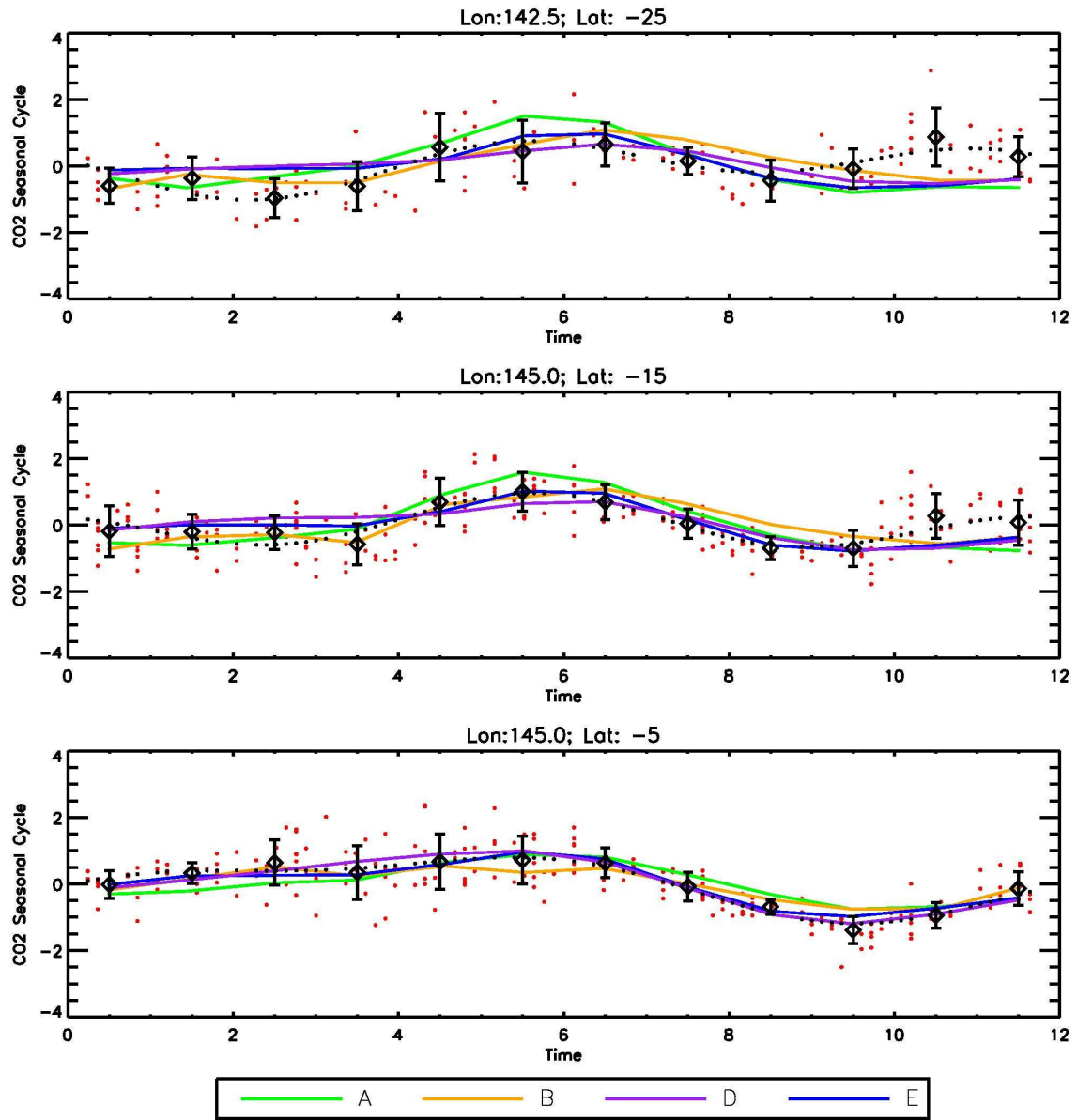


Figure 6:

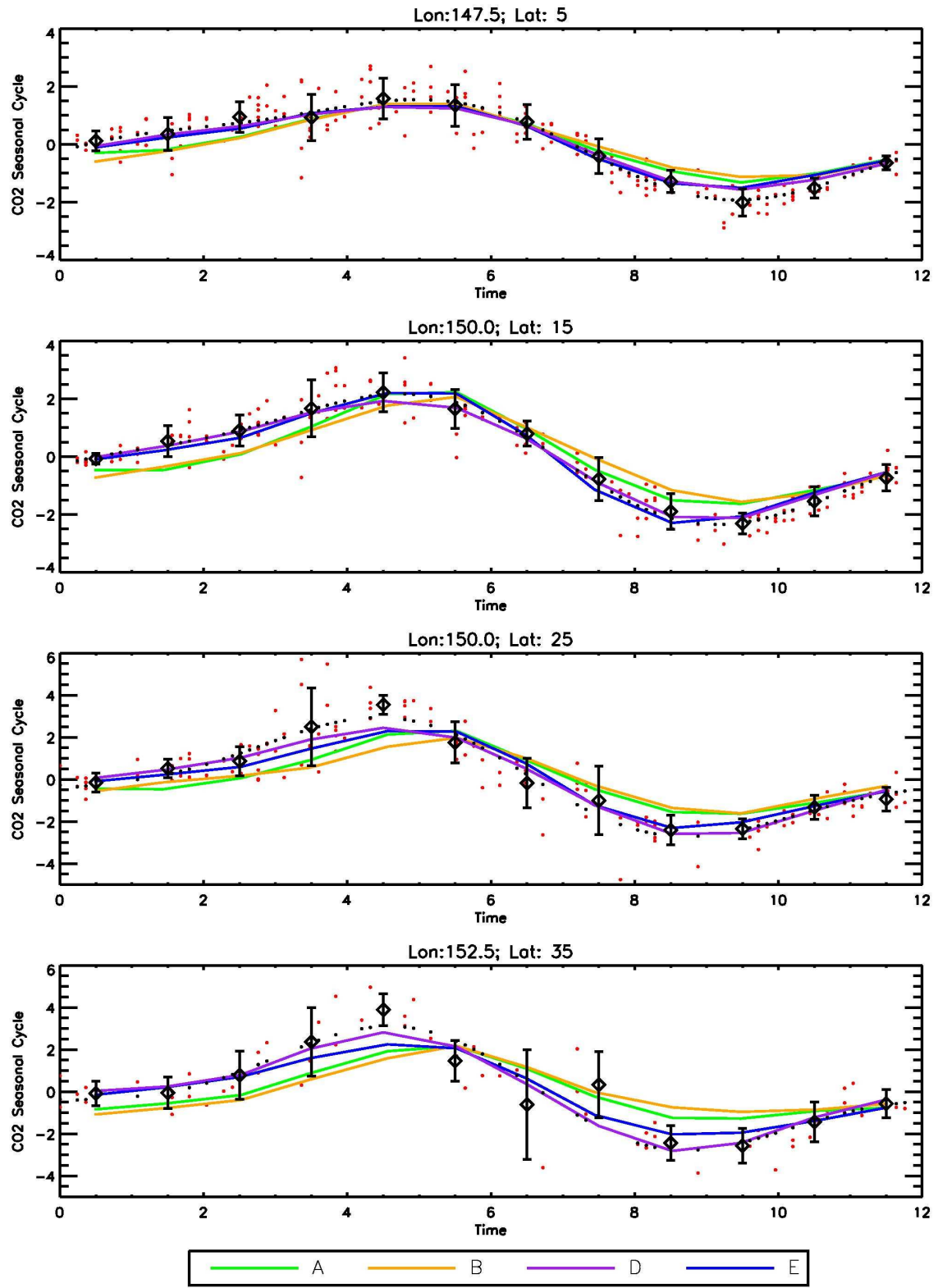


Figure 7:

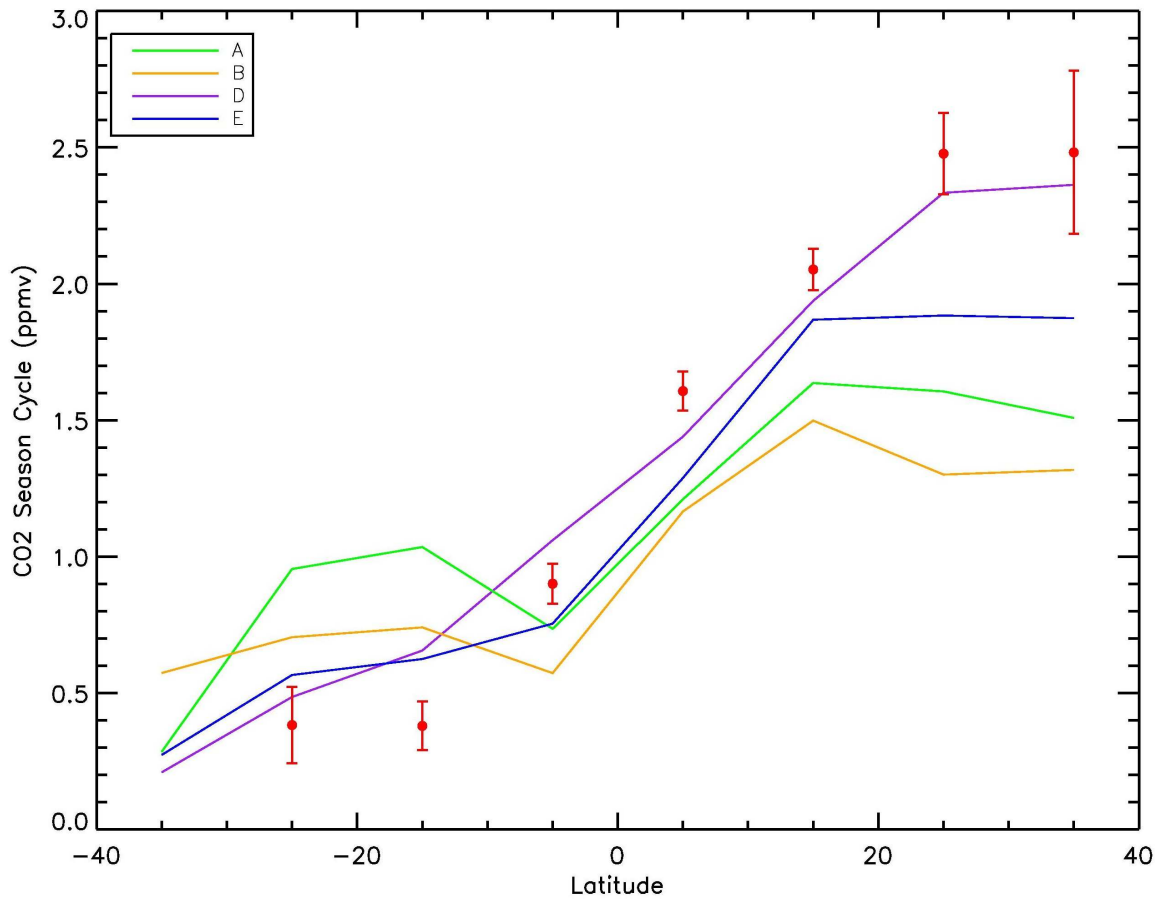


Figure 8:

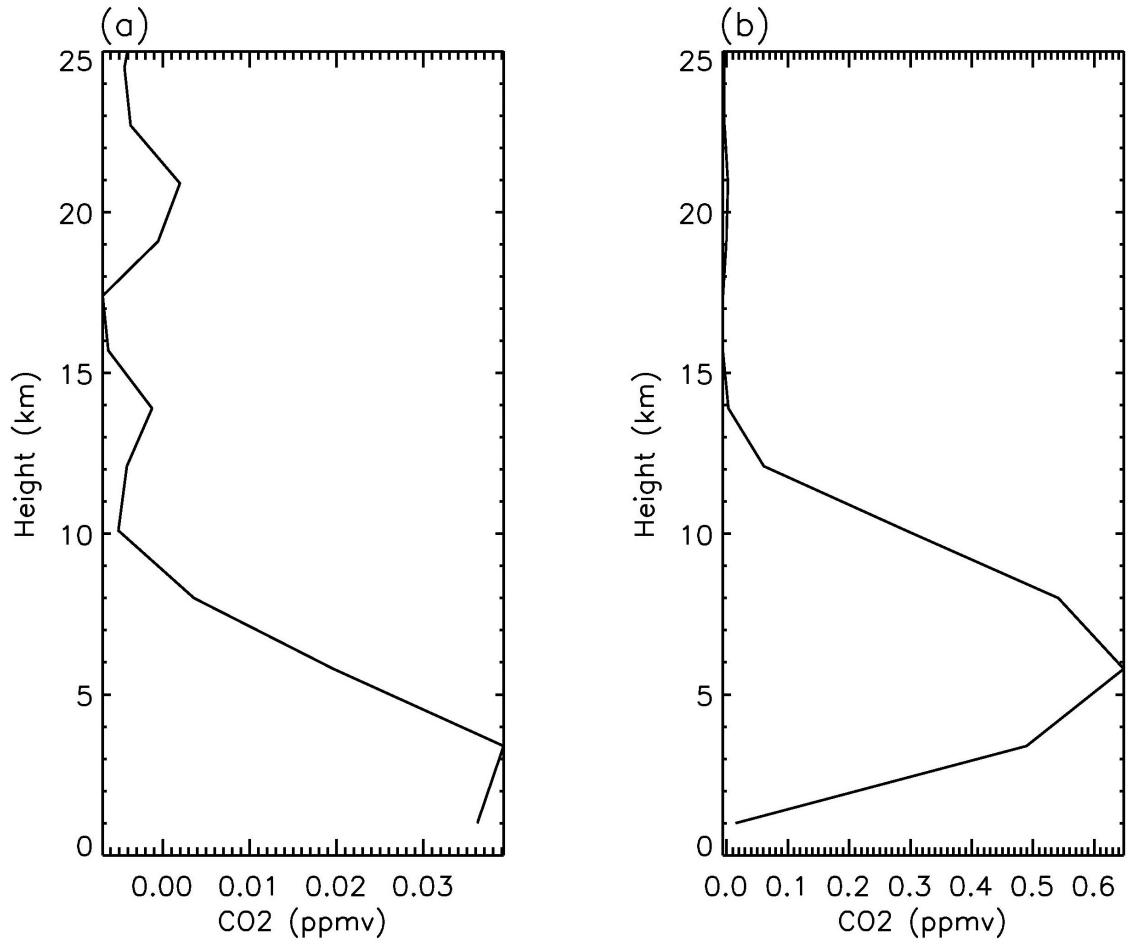


Figure 9:

